Virologica Sinica 39 (2024) 917–928

Contents lists available at ScienceDirect

Virologica Sinica

journal homepage: www.keaipublishing.com/en/journals/virologica-sinica
www.virosin.org

Research Article

Efficient and robust reverse genetics system for bovine rotavirus generation and its application for antiviral screening

Song-Kang Qin [a,b,1], Kuan-Hao Li [a,1], Ben-Jin Liu [a,1], Cun Cao [a], De-Bin Yu [a], Zhi-Gang Jiang [a], Jun Wang [a], Yu-Xin Han [a], Fang Wang [a], Ying-Lin Qi [a], Chao Sun [a], Li Yu [a], Ji-Tao Chang [a,c,*], Xin Yin [a,*]

[a] State Key Laboratory for Animal Disease Control and Prevention, Harbin Veterinary Research Institute, Chinese Academy of Agricultural Sciences, Harbin, 150000, China
[b] Laboratory of Molecular and Cellular Epigenetics, Grappe Interdisciplinaire de Génoprotéomique Appliquée, University of Liège, 4000 Liège, Belgium; Molecular Biology, Teaching and Research Center, 5030 Gembloux, Belgium
[c] Institute of Western Agriculture, The Chinese Academy of Agricultural Sciences, Changji, 831100, China

ARTICLE INFO

Keywords:
Bovine rotavirus (BRV)
Optimized reverse genetics system
Reporter virus
High-throughput screen
Small chemical compound

ABSTRACT

Unveiling the molecular mechanisms underlying rotavirus replication and pathogenesis has been hampered by the lack of a reverse genetics (RG) system in the past. Since 2017, multiple plasmid-based RG systems for simian, human, and murine-like rotaviruses have been established. However, none of the described methods have supported the recovery of bovine rotaviruses (BRVs). Here, we established an optimized plasmid-based RG system for BRV culture-adapted strain (BRV G10P [15] BLR) and clinical isolates (BRV G6P [1] C73, G10P [11] HM26) based on a BHK-T7 cell clone stably expressing T7 polymerase. Furthermore, using this optimized RG system, we successfully rescued the reporter virus BRV rC73/Zs, rHM26/Zs and rBLR/Zs, harboring a genetically modified 1.8-kb segment 7 encoding full-length nonstructural protein 3 (NSP3) fused to ZsGreen, a 232-amino acid green fluorescent protein. Analysis of the stability of genomic insertions showed that the rC73/Zs and rBLR/Zs replicated efficiently and were genetically stable in seven rounds of serial passaging, while rHM26/Zs can be stabilized only up to the third generation, indicating that the BRV segment composition may influence the viral fitness. In addition, we adopted the recombinant reporter viruses for high-throughput screening application and discovered 12 candidates out of 1440 compounds with potential antiviral activities against rotavirus. In summary, this improved RG system of BRVs represents an important tool with great potential for understanding the molecular biology of BRV and facilitates the development of novel therapeutics and vaccines for BRV.

1. Introduction

Rotaviruses belong to the *Reoviridae* family, comprising a variety of icosahedral, nonenveloped multi-segmented double-stranded RNA (dsRNA) viruses. Rotaviruses have three concentric layers of proteins that surround an RNA genome, which contains 11 dsRNA segments encoding six structural (VP1 to VP4, VP6, VP7) and six nonstructural (NSP1 to NSP6) proteins. Based on the variability of the VP6 protein, rotaviruses are divided into A–H groups, and group A rotavirus are one of the etiological agents that cause severe diarrhea in mammals and avian host species (Komoto and Taniguchi, 2014). Two viral surface proteins are used to define the rotavirus genotypes including the outer layer protein VP7 for the G genotype and the spike protein VP4 for the P genotype. Currently, at least 42 G and 58 P genotypes have been described for strains isolated from humans and animals worldwide (https://rega.kuleuven.be/cev/viralmetagenomics/virus-classification/rcwg). Notably, the genotypes of circulating strains can change over time and vary by the geographical area of sample collection (Badaracco et al., 2013).

Bovine rotavirus (BRV) is believed to be the most common cause of severe gastroenteritis in calves, resulting in the huge economic losses (Al Mawly et al., 2015; Papp et al., 2013). Currently, G6, G8 and G10, in conjunction with P [1], P [5], P [7] and P [11], are reported to be the common bovine genotypes (Papp et al., 2013) and phenotypes (Badaracco et al., 2012; Collins et al., 2014; Liu et al., 2021; Mohamed et al., 2017; Pourasgari et al., 2016). Moreover, six (G6 I to G6 VI) and ten

* Corresponding authors.
E-mail addresses: yinxin@caas.cn (X. Yin), changjitao@caas.cn (J.-T. Chang).
[1] Song-Kang Qin, Kuan-Hao Li and Ben-Jin Liu contributed equally to this work.

https://doi.org/10.1016/j.virs.2024.09.010
Received 17 May 2023; Accepted 26 September 2024
Available online 29 September 2024

(G10 I to G10 *X*) lineages can be distinguished within the G6 and G10 genotypes, respectively (Cowley et al., 2013; Fritzen et al., 2019; Jamnikar-Ciglenecki et al., 2016; Liu et al., 2021). In China, several G genotypes (G6, G8 and G10) and P genotypes (P [1], P [5], P [7] and P [11]) have been detected in the cattle population (Elkady et al., 2021; Liu et al., 2021; Wei et al., 2013; Yan et al., 2020). However, the reassortment among different genotypes and the molecular biology of BRV need to be further investigated.

Reverse genetics (RG) systems are powerful tools for manipulating viral genomes to better understand the mechanisms underlying viral replication and pathogenesis and to facilitate the development of artificially attenuated vaccines and viral vectors. For rotavirus, an early plasmid-based RG systems that required a helper virus have been exploited to engineer novel replicative recombinant rotaviruses containing a cDNA-derived gene segment (Johne et al., 2016; Komoto et al., 2006; Navarro et al., 2013; Trask et al., 2010; Troupin et al., 2010). However, these systems require strong selection conditions to separate the recombinant rotavirus from a helper virus. To overcome the limitation, an entirely plasmid-based RG system for simian rotavirus strain SA11 was developed, which was based on all eleven SA11 gene segments along with expression plasmids encoding fusion-associated small transmembrane (FAST) and vaccinia virus capping enzymes (Kanai et al., 2017, 2019). After a series of optimization, an 11 plasmid-based RG system for rescuing human rotavirus strains KU and Odelia, murine-like rotavirus strains, and recombinant viruses based on an SA11 genetic backbone was established (Falkenhagen et al., 2019, 2020; Kawagishi et al., 2020; Komoto et al., 2017, 2018, 2019; Philip et al., 2019a, 2019b; Sánchez-Tacuba et al., 2020). However, the utility of these current RG strategies to rescue other rotavirus genotypes and clinical isolates has not been reported yet.

When using the current RG system, we could easily rescue the simian rotavirus SA11 strains, but it was challenging to rescue G6 and G10 BRVs (Table 1), which may be caused by the biological diversity among different species of rotaviruses. Thus, we sought to develop a more reproducible and efficient bovine reverse genetics (BRG) system for rescuing G6 and G10 BRVs. This system relies on an isolated BHK-T7 cell clone characterized by the high T7 polymerase expression and highly transfection efficiency. Utilizing this highly stable system, we successfully rescued culture-adapted BRV strain and two clinical isolates. Besides, we engineered infectious recombinant BRV rBLR/Zs, rC73/Zs and rHM26/Zs strains, which expressed ZsGreen reporters. And then we conducted serological investigations in some regions using rC73/Zs. Finally, we rescued BRV rC73/GLuc which expressed GLuc active enzyme for high-throughput screening. Through this screening, we identified 12 potential small molecule compounds with anti-BRV activity. In summary, our BRG system enables more efficient recovery of some G6 and G10 BRVs, which maybe great additions to the tool for studying the molecular virology of BRV and for developing future next-generation BRV vaccines and expression vectors.

Table 1
Rescue efficiency and repeatability of the rotavirus strains.

Recombinant RV Strain		Rescue efficiency (%)					
		Kanai	Komoto	BHK-T7	BHK-T7-M1	BHK-T7-M2	BHK-T7-M3
Simian	rSA 11	100 (3/3)	100 (3/3)	100 (3/3)	100 (3/3)	100 (3/3)	100 (3/3)
Bovine	rBLR	0 (0/3)	0 (0/3)	60 (6/10)	100 (10/10)	60 (6/10)	100 (10/10)
Bovine	rC73	0 (0/3)	0 (0/3)	30 (3/10)	100 (10/10)	20 (2/10)	100 (10/10)
Bovine	rHM26	0 (0/3)	0 (0/3)	20 (2/10)	90 (9/10)	20 (2/10)	80 (8/10)
Bovine	rBLR/Zs	0 (0/3)	0 (0/3)	40 (4/10)	100 (10/10)	50 (5/10)	100 (10/10)
Bovine	rC73/Zs	0 (0/3)	0 (0/3)	30 (3/10)	100 (10/10)	30 (3/10)	80 (8/10)
Bovine	rHM26/Zs	0 (0/3)	0 (0/3)	10 (1/10)	90 (9/10)	20 (2/10)	80 (8/10)

2. Materials and methods

2.1. Cells and viruses

Baby hamster kidney cell line, BHK-T7, constitutively expressing T7 RNA polymerase (was constructed in our laboratory), was cultured in Dulbecco's modified Eagle medium (DMEM, Sigma-Aldrich) supplemented with 10% fetal bovine serum (FBS, PAA) (complete medium). To establish BHK-T7 monoclonal cells, BHK-T7 cells were selected by transfection with an NSP3 reporter gene (NSP3 full-length gene fused with *ZsGreen* gene) containing T7 promoter, followed by sorting the transfected BHK-T7 cells with green fluorescence using flow sorting technology. Monkey kidney cell lines Marc-145 were cultured in complete medium. BRV strain C73 (G6P [1]), HM26 (G10P [11]) and BLR (G10P [15]) were preserved in our laboratory. The viruses were pretreated with 10 μg/mL trypsin (type IX, from porcine pancreas, Sigma-Aldrich) and then propagated in Marc-145 cells in incomplete medium (DMEM supplemented with 5 μg/mL trypsin).

2.2. Sequence determination of BRV strains C73, HM26 and BLR

Viral dsRNAs were extracted from C73, HM26 or BLR virions using Trizol (Invitrogen). Viral genomic cDNAs including intact 5′ and 3′ termini were amplified from viral dsRNA by full-length amplification of cDNA as previously described (Maan et al., 2007). Briefly, a selfpriming oligo DNA linker, C9 anchor primer, was attached to the 3′ ends of viral dsRNAs using T4 RNA ligase (Thermo Fisher Scientific), and adaptor-ligated rotavirus dsRNAs were purified by 1% agarose gel electrophoresis. Purified viral cDNAs were synthesized using ThermoScript reverse transcriptase (Thermo Fisher Scientific). Full-length viral cDNAs were amplified with a single primer complementary to the C9 anchor primer using KOD-Plus-Neo polymerase (Toyobo). Amplified viral cDNAs were subcloned into pBluescript KS (+) and subjected to sequencing. Cycle sequencing reactions were performed using BigDye terminator (Applied Biosystems), and viral sequences were determined on an ABI 3130 genetic analyzer (Life Technologies).

2.3. Plasmid construction

We constructed 11 plasmids of 3 strains based on the vector backbones of pT7/VP1SA11, which was purchased from Addgene plasmid (https://www.addgene.org/Takeshi_Kobayashi). To construct T7-driven plasmids, we used pT7/VP1C73/HM26/BLR, pT7/VP2C73/HM26/BLR, pT7/VP3C73/HM26/BLR, pT7/VP4C73/HM26/BLR, pT7/VP6C73/HM26/BLR, pT7/VP7C73/HM26/BLR, pT7/NSP1C73/HM26/BLR, pT7/NSP2C73/HM26/BLR, pT7/NSP3C73/HM26/BLR, pT7/NSP4C73/HM26/BLR, pT7/NSP5 C73HM26/BLR, and pT7/NSP3-ZsGreenC73/HM26/BLR, each encoding the full-length nucleotide sequence of the corresponding gene segments of C73, HM26 and BLR virus.

2.4. Recovery of recombinant rotavirus from cloned cDNAs

Monolayers of BHK-T7 cells (5×10^5) in 12-well plates were co-transfected with plasmids using 13.5 μL of Lipofectamine™ 3000 transfection reagent per microgram of plasmid DNA, as follows: 0.6 μg of each strain C73/HM26/BLR rescue plasmid pT7/VP1C73/HM26/BLR, pT7/VP2C73/HM26/BLR, pT7/VP3C73/HM26/BLR, pT7/VP4C73/HM26/

BLR, pT7/VP6C73/HM26/BLR, pT7/VP7C73/HM26/BLR, pT7/NSP1C73/HM26/BLR, pT7/NSP3C73/HM26/BLR(pT7/NSP3-ZsGreen C73/HM26/BLR, pT7/NSP3-GlucC73) and pT7/NSP4C73/HM26/BLR, 1.8 μg of pT7/NSP2C73/HM26/BLR and pT7/NSP5 C73HM26/BLR. After 48 h of incubation in FBS-free medium, Marc-145 cells (2×10^5 cells) were added to the transfected cells and cocultured for 48 h in FBS-free medium supplemented with trypsin (1 μg/mL). After incubation, transfected cells were lysed by freeze/thaw, trypsin was added to cell lysates at a final concentration of 10 μg/mL, and the samples were incubated at 37 °C for 1 h to activate infectious rotaviruses. The lysates were then transferred to fresh Marc-145 cells. After adsorption at 37 °C for 1 h, the lysate-adsorbed Marc-145 cells were washed and cultured in FBS-free DMEM supplemented with 5 μg/mL trypsin and incubated at 37 °C for 18 h–48 h.

2.5. Immunofluorescence assays (IFA)

The BRV was diluted 1000 times with DMEM medium, and 100 μL of the diluted virus was inoculated onto a 96-well plate covered with a single layer of Marc-145 cells, incubated for 1 h, then the virus infection solution was discarded and replaced with serum-free DMEM containing 10 μg/mL trypsin for further incubation. After 18 h of inoculation, the inoculum was discarded. The media was aspirated and cells were washed with PBS once. Infected Cells were fixed with 4% Paraformaldehyde (PFA) for 15 min, 100 μL/well and penetrated with 0.2% TritonX-100 for 15 min, 100 μL/well, and then washed with PBS one time. Block the cells with 10% goat serum made in 1% BSA in PBS for 1 h, 200 μL/well. The cells were incubated with primary antibody anti-VP6 (home-made, purified from mouse positive sera with Protein G Sepharose at 5 mg/mL) at a 1:50 dilution, 200 μL/well for 1 h at at 25℃. The cells were washed with PBS for 5 min, 200 μL/well for three times. Then the cells were incubated with the secondary antibody [Goat anti-Mouse IgG (H + L) Highly Cross-Adsorbed Secondary Antibody, Alexa Fluor™ 488, A-11029, Thermo Scientific, USA, 1:1000 dilutions, 200 μL/well] at 25℃ for 0.5 h–1 h. After the last three-time washes, results were measured with an inverted fluorescence microscope (AMG, Denver, CO, USA).

2.6. Western blotting

Cell lysates were harvest in NP40 buffer supplemented with a protease inhibitor cocktail and phosphatase inhibitor. Proteins were resolved in SDS-PAGE and analyzed by antibody as described using the following antibodies and dilutions: Mouse GFP tag Monoclonal antibody (Proteintech, PRC, 1:2000 dilution), Rabbit T7 RNA polymerase Polyclonal antibody (29943-1-AP, Proteintech, PRC, 1:2000 dilution) and Rabbit Beta Actin Polyclonal antibody (20536-1-AP, Proteintech, PRC, 1:5000 dilution). Secondary antibodies were Goat anti-Rabbit IgG (H + L) Secondary Antibody (31460, Thermo Scientific, USA, 1:5000 dilution) or Goat anti-Mouse IgG (H + L) Secondary Antibody (31431, Thermo Scientific, USA, 1:5000 dilution). Protein bands were visualized with Clarity ECL substrate, Amersham Hyperfilm, and a STRUCTURIX X-ray film processor.

2.7. Electrophoretic analysis of viral genomic dsRNA

Viral genomic dsRNAs were extracted from cell cultures using a QIAamp Viral RNA Mini Kit (Qiagen). The extracted viral dsRNAs were subjected to PAGE analysis. The dsRNAs were electrophoresed in 10% polyacrylamide gels for 16 h at 20 mA at room temperature, followed by silver staining to determine the genomic dsRNA migration profiles.

2.8. Replication kinetics of rotavirus

A monolayer of Marc-145 cells was infected with C73, rC73, rC73/Zs, HM26, rHM26, rHM26/Zs, BLR, rBLR, rBLR/Zs viruses at an MOI of 0.01 for multistep growth curves. After adsorption for 1 h at 37 °C, cells were washed twice with phosphate buffered saline (PBS), and the medium was replaced with DMEM supplemented with 5 μg/mL trypsin. Cells were frozen at −80 °C at 12, 24, 36, 48, 60 and 72 h post infection. Virus titers were determined ($TCID_{50}$) using Marc-145 cells. Data are expressed as the mean ± standard deviation (SD) of triplicate samples.

2.9. Virus neutralization tests (VNT)

First, sera were heat-inactivated at 56 °C for 30 min. Sera was then diluted in 2-fold serial dilutions (1:4 to 1:2048) in media (MEM) and tested in triplicate against BRV. Virus equivalent to a 100-tissue culture infectious dose ($TCID_{50}$) was added to each well. Plates containing virus and serum dilutions were incubated for 1 h at 37 °C in 5% CO_2. Marc-145 cells were cultured for 24 h–48 h, washed twice in PBS, then virus and serum dilutions were added to the cell plates and the maintenance fluid was serum-free DMEM containing 5 μg/mL trypsin. Plates were incubated for another 5 days at 37 °C in 5% CO_2. Test results were evaluated using an optical method.

2.10. High-throughput screening of small molecule compounds

Firstly, Marc-145 cells were inoculated onto a 384-well plate at a rate of 8000 cells per well. After 42 h, the cells were washed twice with PBS (pH = 7.2) and added compound 5 μM per well (Supplementary Table S1). After 6 h, each well of cells was inoculated with 0.3 MOI of rC73/GLuc. Subsequently, the cells were placed in a 37 °C incubator and cultured for 24 h. Finally, the cell supernatant was analyzed using Pierce™ Gaussia Luciferase Flash Assay Kit to detect GLuc active enzyme. The data were analyzed by simple linear regression of correlation_Log2FC using Graphpad Prism 10.0 software (GraphPad, La Jolla, CA, USA) (Supplementary Table S2).

2.11. Flow cytometry

To Quantify the size of BHK cells, monolayers of BHK-T7 cells (1×10^6) were scraped off and washed twice with PBS (pH = 7.2). After that, cells were analyzed using an Apogee-A60-Universal (Apogee Therapeutics, USA) according to the manufacturer's instructions. To quantify the transfection efficiency in BHK-T7 cell lines: 2 μg of the pCAGGS-EGFP plasmids was transfected into BHK-T7 cells (1×10^6). After 24 h post-transfection, the cells were scraped off and washed twice with PBS (pH = 7.2). Cells were analyzed using an Apogee-A60-Universal (Apogee Therapeutics, USA) according to the manufacturer's instructions. All data were analyzed by FlowJo_v10.8.1 software (USA) and Graphpad Prism 10.0 software (GraphPad, La Jolla, CA, USA).

2.12. Plaque formation assay

Briefly, 200 μL of serial 10-fold virus dilutions in Opti-MEM were used to infect cells (1×10^5 /well) seeded in 12-well plates. After the incubation, the viral inoculums were removed, and the cells were covered with a 1% agarose overlay in a serum-free medium supplemented with 5 μg/mL of trypsin. The cultures were then maintained for 5 days at 37 °C. Subsequently, the cultures were fixed using a 10% formaldehyde solution and stained with a 20% crystal violet solution (Sigma-Aldrich, USA) to visualize the plaques formed.

2.13. Statistical analysis

Except for special needs, The data were analyzed by one-way ANOVA or *t*-tests using the Graphpad Prism 10.0 software (GraphPad, La Jolla, CA, USA) and were presented as means ± standard deviation (mean ± SD). The significance level was declared at ns, $P > 0.05$, $^*P < 0.05$, $^{**}P < 0.01$, and $^{***}P < 0.001$.

3. Results

3.1. Establishment of reverse genetics systems for BRV strain BLR

To develop a RG system for BRV, whole-genome accurate sequences of all 11 gene segments of a culture-adapted strain BLR were amplified by using the method of a Full-Length Amplification of cDNAs (FLAC) (Maan et al., 2007). Next, cDNAs encoding each of the 11 dsRNA gene segments were introduced into plasmids at sites flanked by the T7 promoter and hepatitis delta virus (HDV) ribozyme (Rib) sequences (Fig. 1A). Then, we transfected all these 11 plasmid collection into BHK-T7 cells as described previously with some modifications (Kanai et al., 2017, 2019). Twenty-four hours post-transfection, Marc-145, a clone of the African monkey kidney (MA-104) cell line that efficiently support rotavirus infections was added. Three days later, the cells were subjected to three cycles of freezing and thawing and lysates were passaged in Marc-145 cells. Two to three days after the first passage, a significant cytopathic effect (CPE) was observed in Marc-145 cells, suggesting successful recovery of recombinant strain rBLR derived from cloned cDNAs. Indirect immunofluorescence assay (IFA) was further used to determine the specificity of the rBLR, the results showed that the rBLR have obvious green fluorescence with their specific antibodies (Fig. 1B). Electropherotypes of dsRNA purified from BLR and rBLR showed that the 11 genes of rBLR are same as BLR, and rBLR can be stably passaged for at least 10 generations without any significant loss of large gene segments (Fig. 1C). To exclude the possibility that the rBLR preparation was contaminated by the parental BLR strain. As a genetic marker, a unique *Eco*RI site was erased in the *NSP3* gene segment of rBLR by the introduction of a silent mutation A to G at nucleotide position 409. RNA genomes from BLR and rBLR virions were extracted, the complete *NSP3* gene segment was amplified. Sequence analysis demonstrated that the corresponding marker gene segment from the rBLR possessed the introduced mutation at nucleotide position 409, whereas the corresponding gene amplified from the wild-type virus did not (Fig. 1D). Furthermore, the PCR amplicon from wild-type virus BLR as digested by *Eco*RI resulted in two fragments, whereas that from the rBLR was not (Fig. 1D). To confirm whether rBLR have the characteristics of the BLR, we examined the replication kinetics of BLR and rBLR in Marc-145 cells. We found that rBLR replicated as well as the parental BLR (Fig. 1E). These data suggested that rBLR were rescued successfully from cloned cDNAs, and its replication characteristics of rBLR was similar with the wild type strain.

3.2. Optimization of BRV reverse genetic system based on BHK-T7 cells

Although we successfully rescued the BLR strain following the protocol described previously, the efficiency was quite low (Table 1). Since

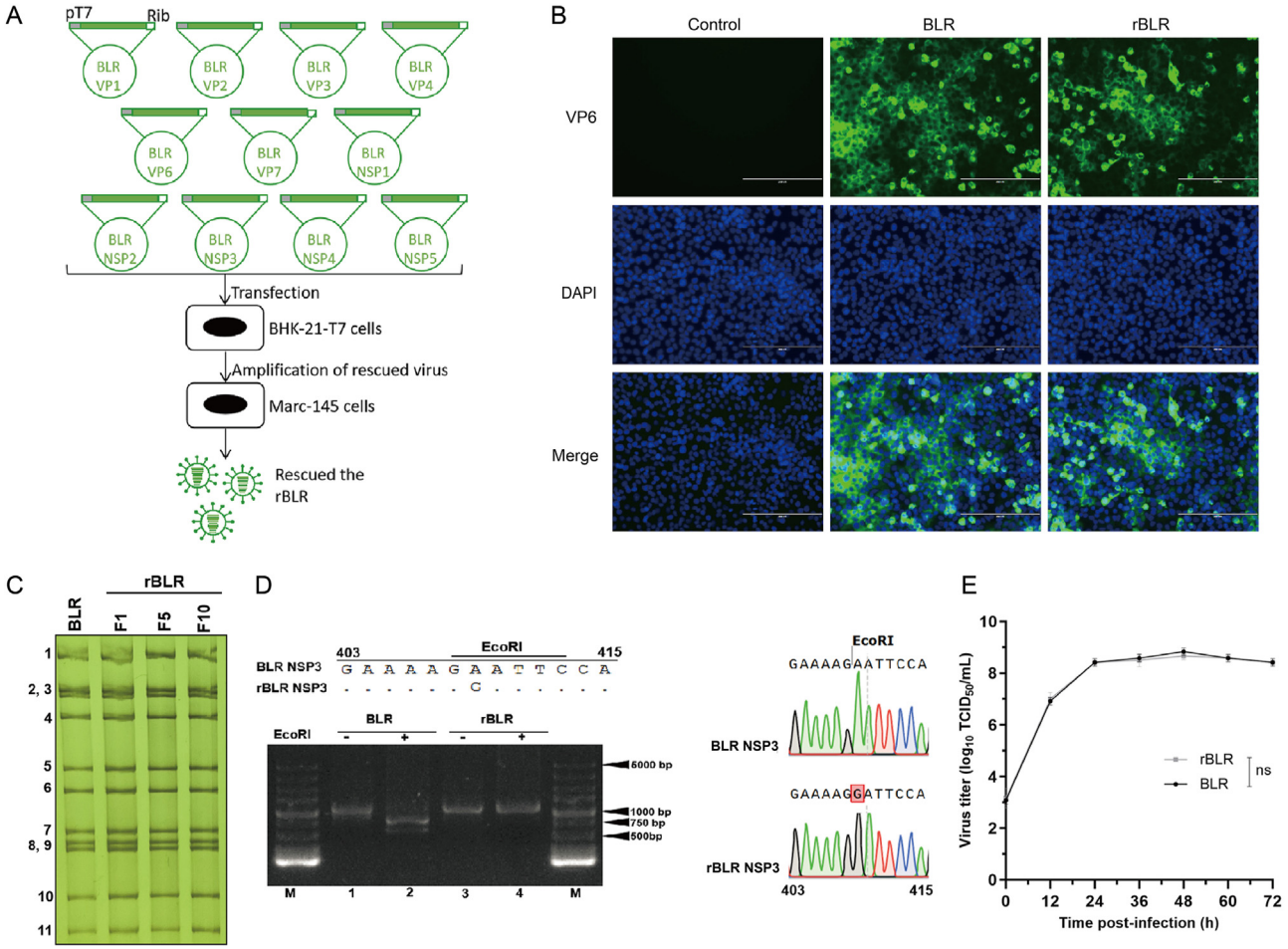

Fig. 1. Establishment of reverse genetics system for BRV strain BLR. **A** Schematic presentation of an 11-plasmid RG system to generate recombinant rBLR. The 11 rescue T7 plasmids encode the full-length segment cDNA of an individual gene of rotavirus, flanked by the T7 RNA polymerase promoter (pT7) and the HDV ribozyme (Rib). To generate rBLR, BHK-T7 cells were cotransfected with the 11 rescue T7 plasmids with 3-fold increased amounts of the two plasmids carrying the NSP2 and NSP5 genes. rBLR was rescued from the cultures of the transfected BHK-T7 cells, followed by amplification on Marc-145 cells. **B** Indirect immunofluorescence (IFA) identification showed that the rBLR reacted with BRV VP6 antibody, scale = 200 μm. **C** Electropherotypes of dsRNA purified from BLR and rBLR(F1, F5 and F10). **D** Electrophoretic of the amplified NSP3 products of BLR and rBLR were treated with *Eco*RI and sequence analysis of the amplified NSP3 products of BLR and rBLR. **E** Cells were infected with BLR or rBLR at a multiplicity of infection (MOI) of 0.01. Cells were frozen at −80 °C at 0, 12, 24, 36, 48, 60 and 72 h post-infection. Virus titers were determined ($TCID_{50}$) using Marc-145 cells. Data are expressed as the mean and standard deviation (SD) of triplicate samples.

the formation of the infectious viral particles is completely dependent on co-existence of all the required viral components in one single transfected BHK-T7 cells. We reasoned that the usage of BHK-T7 clone characterized by the high T7 polymerase expression and highly amenable to transfection would enhance the recovery efficiency. To this end, we performed the single cell cloning to isolate the BHK-T7 clones via FACS sorting. Out of a total of 192 cell clones isolated, only 24 cell clones ultimately survived. By evaluation of the rescue efficiency of BRV BLR strain, we found that the clone BHK-T7-M1 cells brought the highest successful ratio for all tested strains (Table 1). After transfecting an equal amount of pT7/NSP3-ZsGreen BLR plasmid in which the ZsGreen expression was driven under the T7 promoter into BHK-T7 parental cells and three derived clones (BHK-T7-M1, M2, M3), we found that BHK-T7-M1 cells produced significantly more green fluorescence than BHK-T7 and BHK-T7-M2 cells, and slightly more than BHK-T7-M3 cells (Fig. 2A), indicating that BHK-T7-M1 either expresses a high abundance of T7 RNA polymerase or is amendable to transfection. Furthermore, we found that BHK-T7-M1 cells expressed more T7 RNA polymerase than the BHK-T7 and BHK-T7-M2 cells by western blots (Fig. 2B), which might be the key to explain the higher transfection efficiency and rescue efficiency. Upon transfection of eGFP plasmids into these BHK-T7 clones, the most robust eGFP expression and the highest count of fluorescent cells (30.5 ± 1.4%) were notably present in BHK-T7-M1 cells (Fig. 2C–E), indicating the high transfection efficiency of BHK-T7-M1. Interestingly, we also found that the cell morphology of different monoclonal cells varies. In comparison to the parental BHK-T7 cells, both the individual cell size and the mean spectrophotometric area light scatter (SALS) of BHK-T7-M1 and BHK-T7-M3 cells were found to be larger (Fig. 2F and G). Interestingly, despite the increased cell size, there was no discernible impact on their growth rate (Fig. 2H). We speculated that these larger cells may have the capacity to accommodate more plasmids, potentially leading to enhanced rescue efficiency. In conclusion, the identification of an isolated BHK-T7-M1 cell clone proved pivotal in assessing the rescue efficiency of the BRV.

3.3. Rescue of BRV clinical isolates C73 and HM26

To further validate the efficiency of the optimized system, we selected two strains of bovine rotavirus isolated from clinical samples, namely C73 (G6 genotype) and HM26 (G10 genotype) for rescue (Fig. 3A). By following the described protocol above, we successfully obtained the infectious viral particles by transfection of the plasmid collection into BHK-T7-M1 cells. We found that rC73 and rHM26 exhibited similar cellular lesions and fluorescence to their parental strains (Fig. 3B). Electrotypes of dsRNA results showed that both rC73 and rHM26 can be stably inherited for at least 10 generations without any significant loss of large gene segments (Fig. 3C and D). Furthermore, the unique *Hind*III site engineered into the *NSP3* gene segment of rC73 and unique *Sca*II site engineered into the *VP4* gene segment of rHM26 were detected, respectively, indicating that there is no contamination of rC73 and rHM26 by wild type (Fig. 3E and F). Replication kinetics analysis showed that the replication characteristics of rC73 and rHM26 are similar to those of C73 and HM26 (Fig. 3G and H). Collectively, these results demonstrated that our optimized system was suitable for rescuing BRV clinical isolates without any other helper plasmids.

3.4. Generation of stable recombinant BRV expressing reporter fused NSP3-ZsGreen

Engineered recombinant viruses expressing reporter genes have been developed for real-time monitoring of replication and for mass screening of antiviral inhibitors. Previously, several strategies were used to develop the recombinant reporter rotaviruses that expressed red or green fluorescent proteins (FPs) (Kanai et al., 2017, 2019; Komoto et al., 2018; Philip et al., 2019b). After confirming the efficient generation of recombinant BRVs using our optimized 11-plasmid system, we attempted to utilize this robust and simplified reverse genetics system to engineer recombinant BRVs expressing the full-length exogenous proteins. To this end, modified pT7 vectors for segment 7 of rC73 (pT7/NSP3-ZsC73), rHM26 (pT7/NSP3-ZsHM26) and rBLR (pT7/NSP3-ZsBLR) that expressed NSP3 with a fluorescent tag were constructed. The C terminus of the NSP3 ORF in pT7/NSP3 was fused to the ORF for ZsGreen, a 232-amino acid green fluorescent protein. A self-cleaving 2A peptide sequence from porcine teschovirus (2A) was introduced between the NSP3 and ZsGreen ORF (Fig. 4A). After that, these three reporter viruses were rescued following the protocol as described above. A few days after the first passage, a significant cytopathic effect (CPE) and green fluorescence were observed in Marc-145 cells (Fig. 4B), suggesting successful recovery of recombinant strain rC73/Zs, rHM26/Zs and rBLR/Zs derived from cloned cDNAs. The RNA electrophoresis results showed that the *NSP3/Zs* gene of rBLR/Zs, rC73/Zs, and rHM26/Zs were located between the fourth and fifth segments of rBLR, rC73, and *rHM26* genes. While the *NSP3* genes of rBLR, rC73, and rHM26 are located in the eighth segment in the gel (Fig. 4C). In addition, the viral genomic dsRNAs extracted from the rescued viruses, and the complete *NSP3/NSP3-ZsGreen* genes were amplified, the results showed that the PCR products (1074 bp) of NSP3 segments of the rC73, rHM26 and rBLR migrated faster than that of the reporter viruses rC73/Zs, rHM26/Zs and rBLR/Zs as expected (Fig. 4D), which was consistent with the results of RNA electrophoresis. To assess the replication kinetics of the rescued reporter viruses, multiple-step growth curves for rC73, rHM26, rBLR, rC73/Zs rHM26/Zs and rBLR/Zs were determined after infection of Marc-145 cells at a low multiplicity of infection (MOI) of 0.01. Viral titers of the rBLR/Zs and rC73/Zs had no significant difference than that of the parental rBLR (Fig. 4E) and rC73 (Fig. 4F), while viral titer of the rHM26/Zs was significantly lower than that of the parental rHM26 (Fig. 4G). This indicated that the influence of *ZsGreen* gene on the replication characteristics of strains might be strain specific. Overall, we generated recombinant BRV rBLR/Zs, rC73/Zs and rHM26/Zs which can express the ZsGreen fluorescent gene.

3.5. NSP3 gene was one of the factors affecting the stable passage of ZsGreen gene

To examine the stability of BRV-expressing reporter genes, we used monoclonal rBLR/Zs, rC73/Zs, and rHM26/Zs selected by plaque cloning as the first generation, and then serially passaged rC73/Zs, rHM26/Zs and rBLR/Zs in Marc-145 cells. Interestingly, the rC73/Zs and rBLR/Zs expressing fluorescence remained genetically stable during serial passages (at least seven generation) (Fig. 5A and B), but at the fourth generation, the ZSGreen fluorescence was completely lost in rHM26/Zs (Fig. 5C). The results of RNA electrophoresis showed that the *NSP3/Zs* gene located between the fourth and fifth genes has been lost in the fourth generation of rHM26/Zs (Fig. 5C). To investigate the causes of this phenomenon, we replaced the *NSP3/Zs* genes of C73 and HM26, and then rescued the recombinant strain rC73/HN3/Zs with the *NSP3/Zs* gene of HM26 along with the recombinant strain rHM26/C73N3/Zs with the *NSP3/Zs* gene of C73. After passage of rC73/HN3/Zs and rHM26/C73N3/Zs, we found that the *NSP3/Zs* genes of rC73/HN3/Zs could still be stably passaged to the seventh generation (Fig. 5D), and the *NSP3/Zs* genes of rHM26/C73N3/Zs could still express a large amount of green fluorescence in the fifth generation (Fig. 5E). RNA electrophoresis also showed that the passage of rHM26/C73N3/Zs is more stable than rHM26/Zs (Fig. 5C–E). The above results indicated that the stability of the inserted gene was determined by the virus strain, and the *NSP3* gene is one of the key factors affecting the stable passage of the *ZsGreen* gene.

3.6. Application of reporter virus in detection of BRV serum neutralizing antibody

To further demonstrate the utility of this stable BRV reporter expression system, we used rC73/Zs to measure the BRV neutralizing antibody in cattle serum collected from the herd in combination. After the optimization of the serum dilution fold and the viral titer for the high-

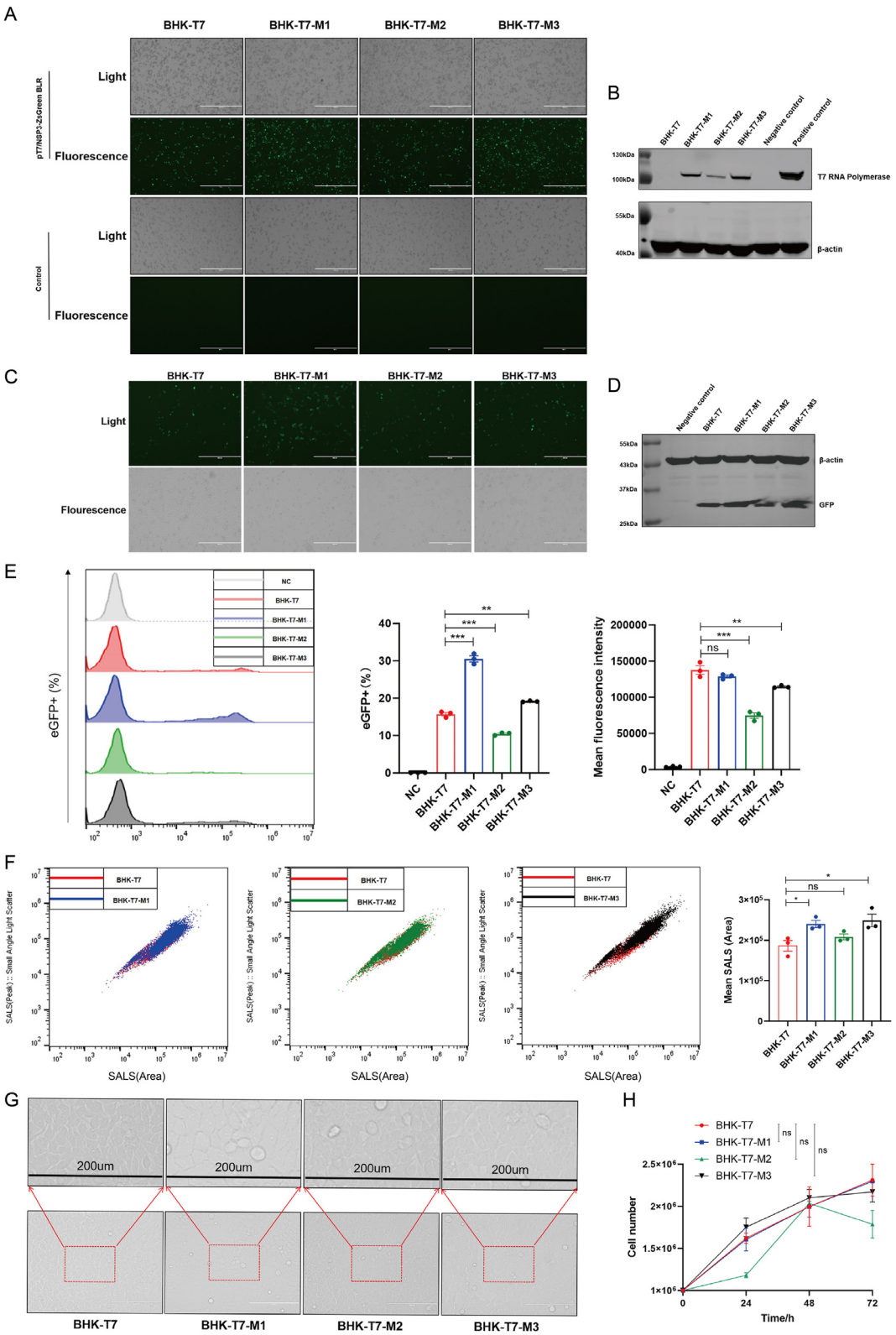

Fig. 2. BHK-T7 cells was the key to determining the efficiency of BRV rescue. **A** The pT7/NSP3-ZsGreen BLR plasmid (2 μg) was transfected into BHK-T7 cells and their monoclonal cells M1, M2, and M3, respectively. After 48 h, they were observed under an inverted fluorescence microscope, scale = 400 μm. **B** Western blot of BHK-T7 cells and its monoclonal cells (BHK-T7-M1, BHK-T7-M2 and BHK-T7-M3) were performed with anti-T7 RNA polymerase antibody. **C–E** The pCAGGS/EGFP plasmid (2 μg) was transfected into BHK-T7 cells and their monoclonal cells M1, M2, and M3, after 24 h, they were observed under an inverted fluorescence microscope (**C**) and were detected EGFP which analyzed by Western blot, scale = 400 μm (**D**) and flow cytometry (**E**). **F** The size of BHK cells was determined using flow cytometry, with BHK-T7 cells serving as a contrl for comparison based on SLAS measurements. **G** Morphology of BHK-T7, BHK-T7-M1, BHK-T7-M2 and BHK-T7-M3 cells under optical microscope, scale = 200 μm. **H** Cells (1×10^6) were seeded onto 12 well plates, and each cell was counted at 0, 24, 48, and 72 h. Data are expressed as the mean and standard deviation (SD) of triplicate samples.

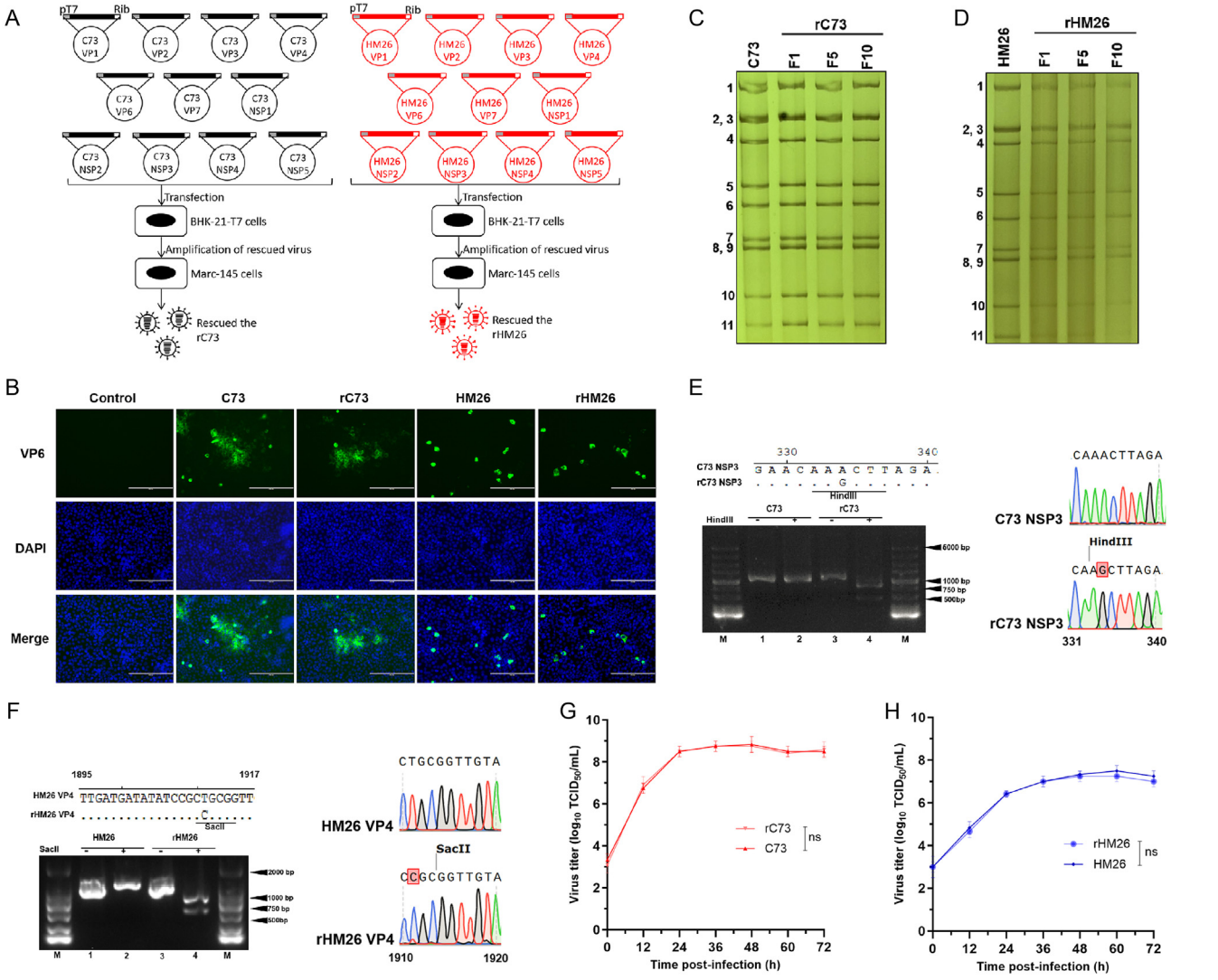

Fig. 3. Establishment of reverse genetics system for BRV clinical isolates. **A** Schematic presentation of an 11-plasmid RG system to generate recombinant rC73 and rHM26. **B** Indirect immunofluorescence (IFA) identification showed that the rC73 and rHM26 reacted with BRV VP6 antibody, scale = 200 μm. **C–D** Electropherotypes of dsRNA purified from (**C**) C73 and rC73(F1, F5 and F10), (**D**) HM26 and rHM26(F1, F5 and F10). **E–F** Electrophoretic analysis of the amplified NSP3 products of C73 and rC73 were treated with *Hind*III and the amplified VP4 products of HM26 and rHM26 were treated with *Sac*II, sequence analysis of the amplified NSP3 products of C73 and rC73 and the amplified VP4 products of HM26 and rHM26. **G–H** Cells were infected virus at a multiplicity of infection (MOI) of 0.01. Cells were frozen at −80 °C at 0, 12, 24, 36, 48, 60 and 72 h postinfection. Virus titers were determined ($TCID_{50}$) using Marc-145 cells. (**G**) C73 and rC73, (**H**) HM26 and rHM26. Data are expressed as the mean and standard deviation (SD) of triplicate samples.

throughput screening using the High Content Imaging Analysis System (Supplementary Fig. S1), we tested 152 bovine serum samples from seven regions in China. The results showed that 146 out of 152 bovine serum samples were positive, with a total positive rate of 96.05% (Fig. 6A, Table 2). There are differences in positive rates and levels among different regions (Fig. 6B). Since there are no commercial vaccines for BRV available in China, the surveillance data indicated that the positive rate of rotavirus infection is relatively high in China, but the proportion of high titer antibodies (greater than or equal to 1:512, data not shown) that can achieve protective levels is relatively low.

3.7. Identification small compounds of anti-BRV infection through a high-throughput small chemical compound screen

Currently, there is no specific drug to treat rotavirus infection. Thus, we established a high-throughput small chemical compound screening assay to determine the antiviral activity of compounds from the L6000-Natural Compound Library (Riva et al., 2021). We modified pT7 vectors for segment 7 of rC73 (pT7/NSP3-GLucC73) that expressed NSP3 with GLuc tag for high-throughput screening (Fig. 7A). The electrophoresis of the dsRNA genome can prove that rC73/GLuc was successfully rescued (Fig. 7B). The viral replication and GLuc activity of C73 and rC73/GLuc in Marc-145 cells indicated that rC73/GLuc can replace C73 in compound screening experiments (Fig. 7C and D). Subsequently, we developed a high-throughput assay to enable large-scale screening of compounds. Specifically, we assessed the potential antiviral activity of 1440 compounds against BRV in Marc-145 cells. Marc-145 cells were pretreated for 6 h with the compounds (5 mM final concentration) and then infected with rC73/GLuc (MOI, 0.3). Twenty-four hours after infection, the supernatants of cell cultures were analyzed by GLuc activity. For each condition, the percentage of infection was calculated as the ratio of GLuc activity in cell supernatant with compound intervention and infected with the rC73/GLuc virus to GLuc activity in cell supernatant without compound intervention and infected with the rC73/GLuc virus (Fig. 7E), MG132 as positive compound control. We observed a reasonable dynamic range between positive and negative controls

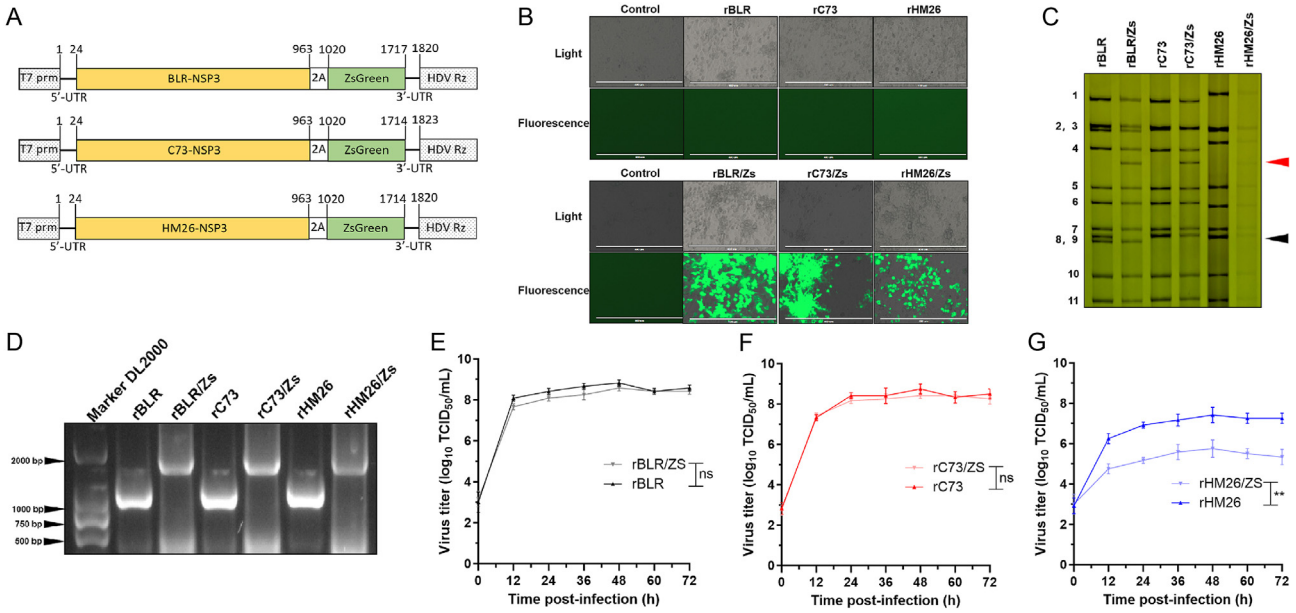

Fig. 4. Generation of recombinant rBLR/Zs, rC73/Zs and rHM26/Zs viruses expressing ZsGreen. **A** Organization of pT7 plasmids expressing NSP3-ZsGreen RNAs, indicating the locations of the T7 promoter (prm) and the hepatitis delta virus (HDV) self-cleaving ribozyme (Rz). Nucleotide positions are labeled. To generate plasmid pT7/NSP3-ZsGreen, the *2A-ZsGreen* gene was inserted after the ORF of the *NSP3* gene. **B** Expression of ZsGreen from rC73/Zs, rHM26/Zs and rBLR/Zs. Marc-145 cells were infected with rC73/Zs, rHM26/Zs and rBLR/Zs at a MOI of 1 and incubated for 24 h, and then expression of ZsGreen in infected cell, was assessed under a bright-field and fluorescence microscope using specific filters, scale = 400 μm. **C** Electropherotypes of dsRNA purified from rBLR, rBLR/Zs, rC73, rC73/Zs, rHM26 and rHM26/Zs. **D** NSP3 PCR of viral dsRNAs extracted from the rC73, rC73/Zs, rHM26, rHM26/Zs, rBLR and rBLR/Zs. **E–G** Replication kinetics of the rBLR and rBLR/Zs (**E**), rC73 and rC73/Zs (**F**), rHM26 and rHM26/Zs (**G**). Monolayers of Marc-145 cells were infected with rotavirus at an MOI of 0.01 and incubated in the presence of trypsin (5 μg/mL) for various times. After freezing/thawing, the viral titer in cell lysates was determined by $TCID_{50}$. Results are expressed as the mean viral titer from triplicate experiments. Error bars denote the SD.

(Fig. 7F) and a positive correlation between replicates (R^2 = 0.79) (Fig. 7G), enabling the identification of compounds with potential antiviral activities. Typically, drugs with therapeutic dose ranges exhibit a half maximal inhibitory concentration (IC_{50}) below 1 μM. In our study, we initially screened compounds with an inhibition rate exceeding 90% on rC73/GLuc in two trials and subsequently performed a dose-response analysis on them. The cytotoxicity of these compounds was evaluated using CCK-8, revealing that 10 compounds had an IC_{50} below 1 μM (Fig. 8). Additionally, based on the CCK-8 cell viability testing results, the 50% cytotoxic concentration (CC_{50}) of these 12 compounds was determined to be greater than 5 μM (Fig. 8). Furthermore, we confirmed the inhibitory effect of these 12 compounds on C73 at a concentration of 1 μM through plaque assays, yielding consistent outcomes (Supplementary Fig. S2). These findings suggest that the impact of these compounds on viral replication occurs at concentrations significantly higher than those affecting cell viability, indicating that their antiviral effects are not confounded by cytotoxicity concerns.

4. Discussion

An entirely plasmid-based reverse genetics (RG) system was already developed for rotavirus. However, current research indicated that the system is applicable to simian, human, and murine-Like rotaviruses (Sánchez-Tacuba et al., 2020). Currently, there is no RG system suitable for bovine rotavirus. Based on this point, we established a reverse genetic system for G6 and G10 BRVs, which not only helped us successfully rescue the cell culture adaptive strain BLR, but also rescued clinically isolated strains C73 and HM26. rBLR, rC73 and rHM26 grew quite efficiently in Marc-145 cell lines and genetically stable which were similar with wild type strains BLR, C73 and HM26.

Rescue efficiency is one of the critical parameters for evaluating the reverse genetic systems. The co-expression of FAST protein, capping enzyme, and rescue plasmid in BHK-T7 cells can enhance the rescue efficiency of rotavirus (Kanai et al., 2017). Additionally, co-transfection of C3P3-G1 plasmid with rotavirus plasmids has been employed to achieve higher efficiency (Sánchez-Tacuba et al., 2020). Our findings align with previous reports indicating that BHK-T7 cells significantly influence rescue efficiency (Philip et al., 2020). In contrast to providing specialized nutrients to BHK-T7 cells, we adopted a monoclonal method to select cell clones supporting stable and high rescue efficiency (Philip et al., 2020). Our results demonstrated a positive correlation between rescue efficiency and transfection efficiency in BHK-T7 cells, which was also associated with the expression level of T7 RNA polymerase (Fig. 2B). Furthermore, we observed distinct cell morphology differences between high and low rescue efficiency cells (Fig. 2F and G), suggesting that larger cells may facilitate increased plasmid entry and, subsequently, higher rescue efficiency. Thus, BHK-T7 cells play a pivotal role in determining rescue efficiency.

Several naturally occurring rotavirus mutants possess genome segments of unusually large size due to intragenic sequence duplications, particularly NSP1 and NSP3 segments (Arnold et al., 2012; Desselberger, 2020; Hundley et al., 1985; Patton et al., 2001), It have also been noted for segments encoding NSP2, NSP4, NSP5, and VP6 (Ballard et al., 1992; Gault et al., 2001; Kojima et al., 1996; Shen et al., 1994). These findings highlight the rotavirus genome's ability to accommodate significant amounts of additional genetic material. Subsequent findings showed that rotaviruses can be molecularly engineered to function as plug-and-play expression vectors capable of driving the production of a separate heterologous protein without affecting the function of the rotaviral NSP3 protein (Diebold et al., 2022; Philip and Patton, 2020, 2022). We successfully established BRVs expressing fluorescent (ZSGreen) and bioluminescent (GLuc) reporters. However, stability issues were encountered, particularly with the HM26 strain expressing ZSGreen, suggesting an influence of the *NSP3* gene on reporter gene stability. Interestingly, the rC73/Zs and rBLR/Zs expressing reporters remained genetically stable during serial passages, but at the 4th generation, the ZSGreen protein

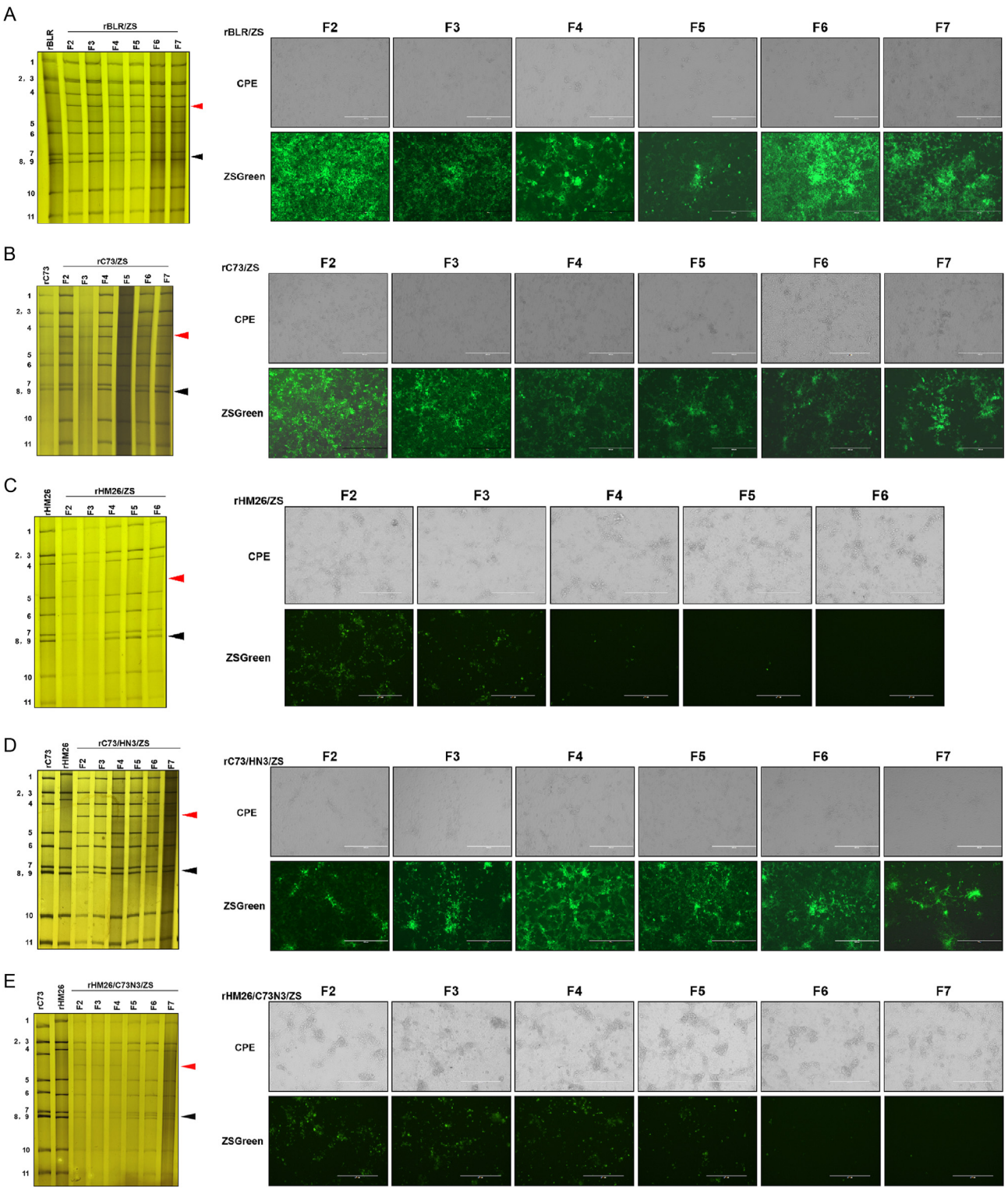

Fig. 5. Electrophoresis of the dsRNA genome, CPE and fluorescence purified from filial 2 (F2) to F6/F7 viruses was examined, scale = 400 μm. **A** rBLR/ZS; **B** rC73/ZS; **C** rHM26/ZS; **D** rC73/HN3/ZS; **E** rHM26/C73N3/ZS; The positions of NSP3-ZsG (ZsGreen) genes and wild-type *NSP3* genes are indicated by red arrows and black arrows.

began to be lost in rHM26/Zs. When the *NSP3-ZsGreen* gene of C73 were replaced onto HM26, we found that the ZsGreen protein was still expressed in the fifth generation, indicating that the *NSP3* gene affects the stability of ZsGreen protein expression. Unfortunately, we have not yet found a method to enable stable inheritance of rHM26/Zs, which need further investigation.

The conventional neutralization test for rotavirus was time-consuming, often requiring a significant amount of time to observe the result. Additionally, the criteria used to determine the outcome of the test were often subjective. Therefore, a high-throughput neutralization assay was developed using the stable rC73/ZsGreen strain, facilitating the investigation of rotavirus infection across seven regions in China. This

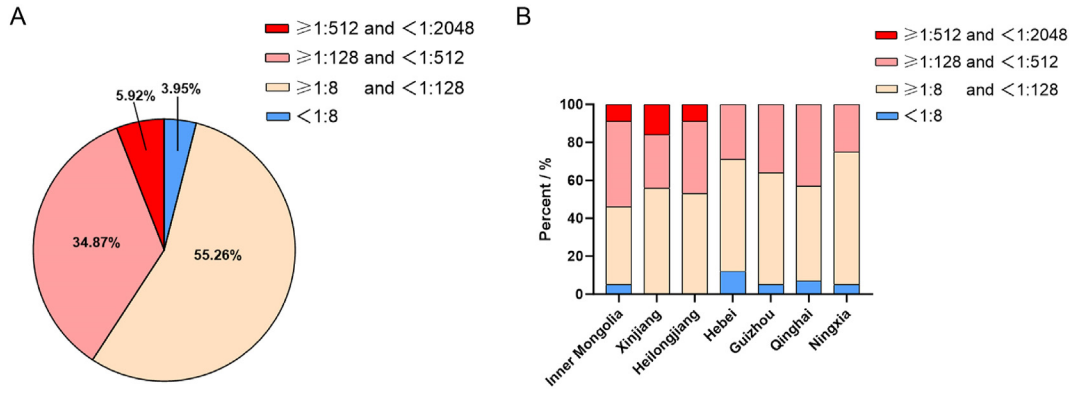

Fig. 6. Detecting for neutralizing antibodies specific for BRV in bovine sera. **A** The proportion of positive levels in 152 bovine serum samples. **B** The proportion of positive levels in bovine serum samples from different regions. Negative (lower than 1:8), low neutralization titer (greater than or equal to 1:8, lower than 1:128), medium neutralization titer (greater than or equal to 1:128, lower than 1:512), high neutralization titer (greater than or equal to 1:512, lower than 1:2048).

Table 2
Seroprevalence of BRV virus in China in different regions.

Region	Sample size	Negative	Low neutralization titer	Medium neutralization titer	High neutralization titer	Seroprevalence	Seroprevalence of high neutralization titer
Inner Mongolia	22	1	9	10	2	95.45%	9.09%
Xinjiang	25	0	14	7	4	100.00%	16.00%
Heilongjiang	32	0	17	12	3	100.00%	9.38%
Hebei	17	2	10	5	0	88.24%	0%
Guizhou	22	1	13	8	0	95.45%	0%
Qinghai	14	1	7	6	0	92.86%	0%
Ningxia	20	1	14	5	0	95.00%	0%
Total	152	6	84	53	9	96.05%	5.92%

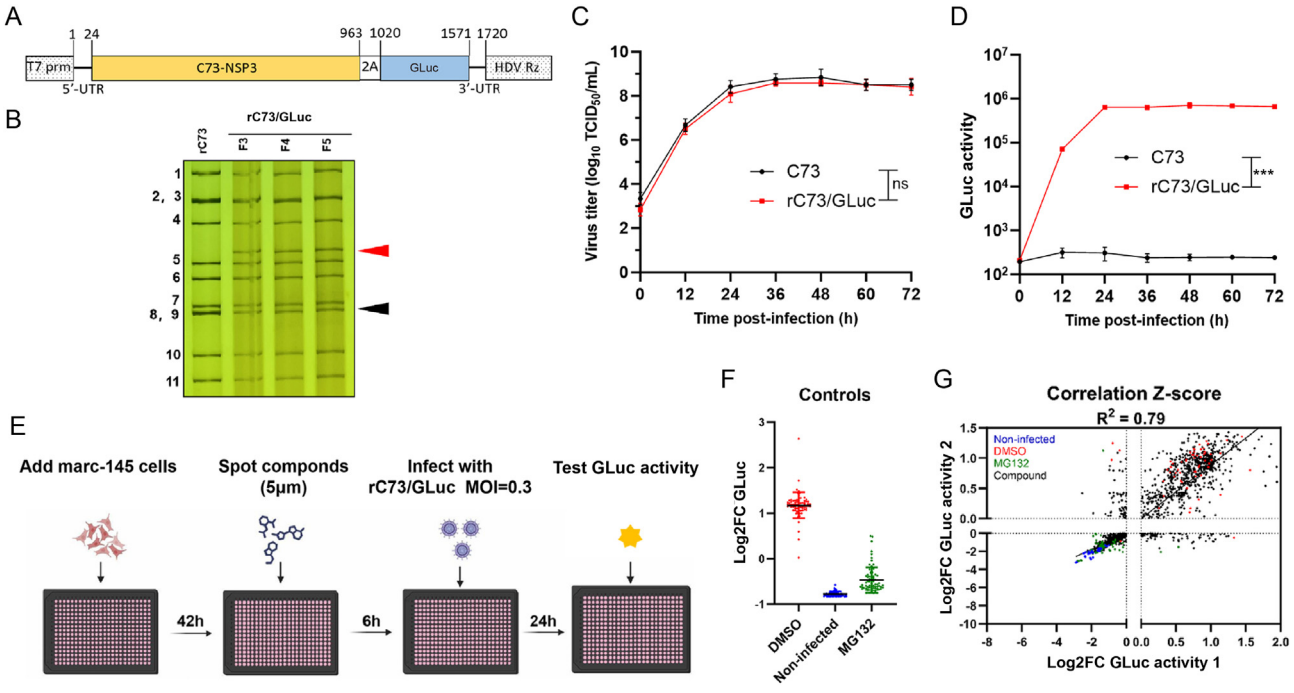

Fig. 7. Identification inhibitors of BRV infection through a high-throughput small chemical compound screen. **A** To generate plasmid pT7/NSP3-GLuc, the 2A-GLuc gene was inserted after the ORF of the *NSP3* gene. **B** Electrophoresis of the dsRNA genome purified from filial 3 (F3) to F5 of rC73/GLuc viruses was examined. **C, D** Viral replication and GLuc activity of C73 and rC73/GLuc in Marc-145 cells. **E** Schematic of the screening strategy used for the identification of chemical compounds showing antiviral activity directed against BRV. Marc-145 cells were pretreated for 6 h with the compounds (5 μM final concentration) and then infected with rC73/GLuc (MOI, 0.3). Twenty-four hours after infection, the supernatants of cell cultures were analyzed by GLuc activity. For each condition, the percentage of infection was calculated as the ratio of GLuc activity in cell supernatant with compound intervention and infected with the rC73/GLuc virus to GLuc activity in cell supernatant without compound intervention and infected with the rC73/GLuc virus. **F** Z-scores after normalization to the median of each plate for all positive (MG132) and negative (DMSO) controls, as well as for non-infected cells, across all the screening plates. Data are mean ± SD. for at least 219 independent wells. **G** Correlation plot indicates the activity (Z-score) of each compound in the two replicate screens.

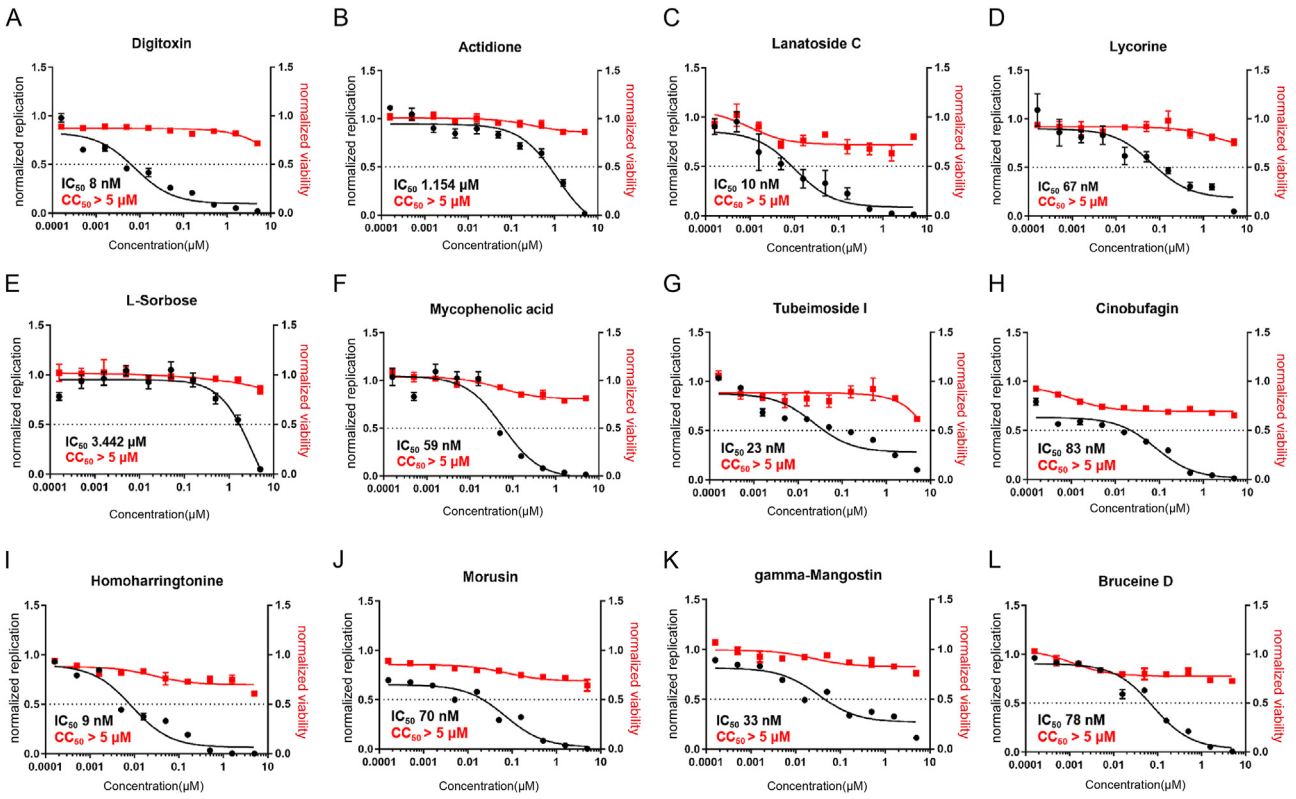

Fig. 8. The IC_{50} and CC_{50} of compounds against BRV infection. **A–L** Marc-145 cells were pretreated for 6 h with decreasing concentrations of compounds and then infected with BRV rC73/GLuc at an MOI of 0.3. Twenty-four hours after infection, the supernatants of cell cultures were analyzed by GLuc activity, cell activity were analyzed by CCK-8. Dose-response curves for infectivity (black) and cell activity (red) are shown. Data are normalized to the mean for DMSO-treated wells and represent means ± SD from n = 3 independent experiments. IC_{50} and CC_{50} for each compound were calculated using a three-parameter logistic nonlinear regression model and are indicated. (**A**) Digitoxin; (**B**) Actidione; (**C**) Lanatoside C; (**D**) Lycorine; (**E**) L-Sorbose; (**F**) Mycophenolic acid; (**G**) Tubeimoside I; (**H**) Cinobufagin; (**I**) Homoharringtonine; (**J**) Morusin; (**K**) gamma-Mangostin; (**L**) Bruceine D.

assay offers a more efficient and objective alternative to traditional neutralization tests. Using this high-throughput neutralization assay, we uncovered the prevalence of rotavirus infection among cattle in seven regions of China. These findings can provide valuable insights for implementing vaccination strategies in cattle herds in China.

Additionally, the establishment of a drug screening method using rC73/GLuc enabled the identification of potential compounds inhibiting bovine rotavirus. The biological properties of rC73/GLuc closely resemble those of C73. Additionally, the GLuc enzyme produced by rC73/GLuc upon virus infection can be released into the cell supernatant, making the detection method more convenient. Notably, this screening approach identified 12 potential inhibitors from a pool of 1440 compounds, providing promising candidates for further investigation. Currently, aside from Mycophenolic acid, which is known to inhibit the IMPDH enzyme leading to nucleotide depletion (Yin et al., 2016). The antiviral mechanisms of other small molecule compounds against rotavirus have not been elucidated. This suggests that our small molecule compound screening system enables not only the validation of known drugs against rotavirus but also the rapid screening for potential novel compounds.

5. Conclusions

In this study, we established a reverse genetics system for BRVs using an isolated BHK-T7 cell clone characterized by high T7 polymerase expression and excellent transfection efficiency. Leveraging this stable system, we successfully rescued multiple BRV strains and generated reporter-expressing recombinant viruses. Additionally, we developed a high-throughput screening assay using reporter BRVs expressing the GLuc active enzyme for the rapid identification of antiviral compounds. Overall, our BRG system offers a valuable tool for studying the molecular virology of BRV and for developing novel treatments.

Data availability

The materials and data presented in this manuscript are available from the corresponding author upon request. The sequence information of BLR, C73, and HM26 has been uploaded to NCBI (BLR VP1-NSP5: PP991467-PP991477; C73 VP1-NSP5: PP991478-PP991488; HM26 VP1-NSP5: PP991489-PP991499) and Science Data Bank (https://doi.org/10.57760/sciencedb.12290).

Ethics statement

This article does not contain any studies with human or animal subjects performed by any of the authors.

Author contributions

Song-Kang Qin: investigation, methodology, data curation, writing-original draft. Kuan-Hao Li: investigation, methodology, validation. Ben-Jin Liu: investigation, methodology, validation. Cun Cao: investigation. De-Bin Yu: validation. Zhi-Gang Jiang: validation, writing-review, funding acquisition. Jun Wang: conceptualization. Yu-Xin Han: conceptualization. Fang Wang: supervision, writing-review. Ying-Lin Qi: supervision, writing-review. Chao Sun: supervision, writing-review. Li Yu: writing-review. Ji-Tao Chang: investigation, methodology, resources, writing-original draft, writing-review & editing. Xin Yin: methodology, funding acquisition, formal analysis, project administration, writing-review & editing.

Conflict of interest

All authors declare that there are no competing interests.

Acknowledgements

The authors would like to thank the members from Yin Laboratory for their critical suggestions. This study was supported by the Heilongjiang Provincial Natural Science Foundation of China (grant no. LH2033C107), the National Key Research and Development Program of China (2023YFD1801302) and the Central Public-interest Scientific Institution Basal Research Fund (grant no. 1610302022010).

Appendix A. Supplementary data

Supplementary data to this article can be found online at https://doi.org/10.1016/j.virs.2024.09.010.

References

Al Mawly, J., Grinberg, A., Prattley, D., Moffat, J., Marshall, J., French, N., 2015. Risk factors for neonatal calf diarrhoea and enteropathogen shedding in New Zealand dairy farms. Vet. J. 203, 155–160.

Arnold, M.M., Brownback, C.S., Taraporewala, Z.F., Patton, J.T., 2012. Rotavirus variant replicates efficiently although encoding an aberrant NSP3 that fails to induce nuclear localization of poly(A)-binding protein. J. Gen. Virol. 93, 1483–1494.

Badaracco, A., Garaicoechea, L., Matthijnssens, J., Louge Uriarte, E., Odeón, A., Bilbao, G., Fernandez, F., Parra, G.I., Parreño, V., 2013. Phylogenetic analyses of typical bovine rotavirus genotypes G6, G10, P[5] and P[11] circulating in Argentinean beef and dairy herds. Infect. Genet. Evol. 18, 18–30.

Badaracco, A., Garaicoechea, L., Rodríguez, D., Uriarte, E.L., Odeón, A., Bilbao, G., Galarza, R., Abdala, A., Fernandez, F., Parreño, V., 2012. Bovine rotavirus strains circulating in beef and dairy herds in Argentina from 2004 to 2010. Vet. Microbiol. 158, 394–399.

Ballard, A., McCrae, M.A., Desselberger, U., 1992. Nucleotide sequences of normal and rearranged RNA segments 10 of human rotaviruses. J. Gen. Virol. 73, 633–638.

Collins, P.J., Mulherin, E., Cashman, O., Lennon, G., Gunn, L., O'Shea, H., Fanning, S., 2014. Detection and characterisation of bovine rotavirus in Ireland from 2006-2008. Ir. Vet. J. 67, 13.

Cowley, D., Donato, C.M., Roczo-Farkas, S., Kirkwood, C.D., 2013. Novel G10P[14] rotavirus strain, northern territory, Australia. Emerg. Infect. Dis. 19, 1324–1327.

Desselberger, U., 2020. What are the limits of the packaging capacity for genomic RNA in the cores of rotaviruses and of other members of the Reoviridae? Virus Res. 276, 197822.

Diebold, O., Gonzalez, V., Venditti, L., Sharp, C., Blake, R.A., Tan, W.S., Stevens, J., Caddy, S., Digard, P., Borodavka, A., Gaunt, E., 2022. Using species a rotavirus reverse genetics to engineer chimeric viruses expressing SARS-CoV-2 spike epitopes. J. Virol. 96, e0048822.

Elkady, G., Zhu, J., Peng, Q., Chen, M., Liu, X., Chen, Y., Hu, C., Chen, H., Guo, A., 2021. Isolation and whole protein characterization of species A and B bovine rotaviruses from Chinese calves. Infect. Genet. Evol. 89, 104715.

Falkenhagen, A., Patzina-Mehling, C., Gadicherla, A.K., Strydom, A., O'Neill, H.G., Johne, R., 2020. Generation of simian rotavirus reassortants with VP4- and VP7-encoding genome segments from human strains circulating in Africa using reverse genetics. Viruses 12, 201.

Falkenhagen, A., Patzina-Mehling, C., Rückner, A., Vahlenkamp, T.W., Johne, R., 2019. Generation of simian rotavirus reassortants with diverse VP4 genes using reverse genetics. J. Gen. Virol. 100, 1595–1604.

Fritzen, J.T.T., Oliveira, M.V., Lorenzetti, E., Miyabe, F.M., Viziack, M.P., Rodrigues, C.A., Ayres, H., Alfieri, A.F., Alfieri, A.A., 2019. Longitudinal surveillance of rotavirus A genotypes circulating in a high milk yield dairy cattle herd after the introduction of a rotavirus vaccine. Vet. Microbiol. 230, 260–264.

Gault, E., Schnepf, N., Poncet, D., Servant, A., Teran, S., Garbarg-Chenon, A., 2001. A human rotavirus with rearranged genes 7 and 11 encodes a modified NSP3 protein and suggests an additional mechanism for gene rearrangement. J. Virol. 75, 7305–7314.

Hundley, F., Biryahwaho, B., Gow, M., Desselberger, U., 1985. Genome rearrangements of bovine rotavirus after serial passage at high multiplicity of infection. Virology 143, 88–103.

Jamnikar-Ciglenecki, U., Kuhar, U., Sturm, S., Kirbis, A., Racki, N., Steyer, A., 2016. The first detection and whole genome characterization of the G6P[15] group A rotavirus strain from roe deer. Vet. Microbiol. 191, 52–59.

Johne, R., Reetz, J., Kaufer, B.B., Trojnar, E., 2016. Generation of an avian-mammalian rotavirus reassortant by using a helper virus-dependent reverse genetics system. J. Virol. 90, 1439–1443.

Kanai, Y., Kawagishi, T., Nouda, R., Onishi, M., Pannacha, P., Nurdin, J.A., Nomura, K., Matsuura, Y., Kobayashi, T., 2019. Development of stable rotavirus reporter expression systems. J. Virol. 93, e01774-18.

Kanai, Y., Komoto, S., Kawagishi, T., Nouda, R., Nagasawa, N., Onishi, M., Matsuura, Y., Taniguchi, K., Kobayashi, T., 2017. Entirely plasmid-based reverse genetics system for rotaviruses. Proc. Natl. Acad. Sci. U. S. A 114, 2349–2354.

Kawagishi, T., Nurdin, J.A., Onishi, M., Nouda, R., Kanai, Y., Tajima, T., Ushijima, H., Kobayashi, T., 2020. Reverse genetics system for a human group A rotavirus. J. Virol. 94, e00963-19.

Kojima, K., Taniguchi, K., Urasawa, T., Urasawa, S., 1996. Sequence analysis of normal and rearranged NSP5 genes from human rotavirus strains isolated in nature: implications for the occurrence of the rearrangement at the step of plus strand synthesis. Virology 224, 446–452.

Komoto, S., Fukuda, S., Ide, T., Ito, N., Sugiyama, M., Yoshikawa, T., Murata, T., Taniguchi, K., 2018. Generation of recombinant rotaviruses expressing fluorescent proteins by using an optimized reverse genetics system. J. Virol. 92, e00588-18.

Komoto, S., Fukuda, S., Kugita, M., Hatazawa, R., Koyama, C., Katayama, K., Murata, T., Taniguchi, K., 2019. Generation of infectious recombinant human rotaviruses from just 11 cloned cDNAs encoding the rotavirus genome. J. Virol. 93, e02207-18.

Komoto, S., Kanai, Y., Fukuda, S., Kugita, M., Kawagishi, T., Ito, N., Sugiyama, M., Matsuura, Y., Kobayashi, T., Taniguchi, K., 2017. Reverse genetics system demonstrates that rotavirus nonstructural protein NSP6 is not essential for viral replication in cell culture. J. Virol. 91, e00695-17.

Komoto, S., Sasaki, J., Taniguchi, K., 2006. Reverse genetics system for introduction of site-specific mutations into the double-stranded RNA genome of infectious rotavirus. Proc. Natl. Acad. Sci. U. S. A 103, 4646–4651.

Komoto, S., Taniguchi, K., 2014. [Rotaviruses]. Uirusu 64, 179–190.

Liu, X., Yan, N., Yue, H., Wang, Y., Zhang, B., Tang, C., 2021. Detection and molecular characteristics of bovine rotavirus A in dairy calves in China. J. Vet. Sci. 22, e69.

Maan, S., Rao, S., Maan, N.S., Anthony, S.J., Attoui, H., Samuel, A.R., Mertens, P.P.C., 2007. Rapid cDNA synthesis and sequencing techniques for the genetic study of bluetongue and other dsRNA viruses. J. Virol. Methods 143, 132–139.

Mohamed, F.F., Mansour, S.M.G., El-Araby, I.E., Mor, S.K., Goyal, S.M., 2017. Molecular detection of enteric viruses from diarrheic calves in Egypt. Arch. Virol. 162, 129–137.

Navarro, A., Trask, S.D., Patton, J.T., 2013. Generation of genetically stable recombinant rotaviruses containing novel genome rearrangements and heterologous sequences by reverse genetics. J. Virol. 87, 6211–6220.

Papp, H., László, B., Jakab, F., Ganesh, B., De Grazia, S., Matthijnssens, J., Ciarlet, M., Martella, V., Bányai, K., 2013. Review of group A rotavirus strains reported in swine and cattle. Vet. Microbiol. 165, 190–199.

Patton, J.T., Taraporewala, Z., Chen, D., Chizhikov, V., Jones, M., Elhelu, A., Collins, M., Kearney, K., Wagner, M., Hoshino, Y., et al., 2001. Effect of intragenic rearrangement and changes in the 3' consensus sequence on NSP1 expression and rotavirus replication. J. Virol. 75, 2076–2086.

Philip, A.A., Dai, J., Katen, S.P., Patton, J.T., 2020. Simplified reverse genetics method to recover recombinant rotaviruses expressing reporter proteins. J. Vis. Exp. https://doi.org/10.3791/61039.

Philip, A.A., Herrin, B.E., Garcia, M.L., Abad, A.T., Katen, S.P., Patton, J.T., 2019a. Collection of recombinant rotaviruses expressing fluorescent reporter proteins. Microbiol. Resour. Announc. 8, e00523-19.

Philip, A.A., Patton, J.T., 2022. Generation of recombinant rotaviruses expressing human norovirus capsid proteins. J. Virol. 96, e0126222.

Philip, A.A., Patton, J.T., 2020. Expression of separate heterologous proteins from the rotavirus NSP3 genome segment using a translational 2A stop-restart element. J. Virol. 94, e00959-20.

Philip, A.A., Perry, J.L., Eaton, H.E., Shmulevitz, M., Hyser, J.M., Patton, J.T., 2019b. Generation of recombinant rotavirus expressing NSP3-UnaG fusion protein by a simplified reverse genetics system. J. Virol. 93, e01616-19.

Pourasgari, F., Kaplon, J., Karimi-Naghlani, S., Fremy, C., Otarod, V., Ambert-Balay, K., Mirjalili, A., Pothier, P., 2016. The molecular epidemiology of bovine rotaviruses circulating in Iran: a two-year study. Arch. Virol. 161, 3483–3494.

Riva, L., Goellner, S., Biering, S.B., Huang, C.-T., Rubanov, A.N., Haselmann, U., Warnes, C.M., De Jesus, P.D., Martin-Sancho, L., Terskikh, A.V., et al., 2021. The compound SBI-0090799 inhibits Zika virus infection by blocking *De Novo* formation of the membranous replication compartment. J. Virol. 95, e0099621.

Sánchez-Tacuba, L., Feng, N., Meade, N.J., Mellits, K.H., Jaïs, P.H., Yasukawa, L.L., Resch, T.K., Jiang, B., López, S., Ding, S., et al., 2020. An optimized reverse genetics system suitable for efficient recovery of simian, human, and murine-like rotaviruses. J. Virol. 94, e01294-20.

Shen, S., Burke, B., Desselberger, U., 1994. Rearrangement of the VP6 gene of a group A rotavirus in combination with a point mutation affecting trimer stability. J. Virol. 68, 1682–1688.

Trask, S.D., Taraporewala, Z.F., Boehme, K.W., Dermody, T.S., Patton, J.T., 2010. Dual selection mechanisms drive efficient single-gene reverse genetics for rotavirus. Proc. Natl. Acad. Sci. U. S. A 107, 18652–18657.

Troupin, C., Dehée, A., Schnuriger, A., Vende, P., Poncet, D., Garbarg-Chenon, A., 2010. Rearranged genomic RNA segments offer a new approach to the reverse genetics of rotaviruses. J. Virol. 84, 6711–6719.

Wei, S., Gong, Z., Che, T., Guli, A., Tian, F., 2013. Genotyping of calves rotavirus in China by reverse transcription polymerase chain reaction. J. Virol Methods 189, 36–40.

Yan, N., Li, R., Wang, Y., Zhang, B., Yue, H., Tang, C., 2020. High prevalence and genomic characteristics of G6P[1] Bovine Rotavirus A in yak in China. J. Gen. Virol. 101, 701–711.

Yin, Y., Wang, Y., Dang, W., Xu, L., Su, J., Zhou, X., Wang, W., Felczak, K., van der Laan, L.J.W., Pankiewicz, K.W., et al., 2016. Mycophenolic acid potently inhibits rotavirus infection with a high barrier to resistance development. Antivir. Res. 133, 41–49.